Neuroscience 298 (2015) 200–210

THETA-FREQUENCY PHASE-LOCKING OF SINGLE ANTERIOR CINGULATE CORTEX NEURONS AND SYNCHRONIZATION WITH THE MEDIAL THALAMUS ARE MODULATED BY VISCERAL NOXIOUS STIMULATION IN RATS

J. WANG, [a,b] **B. CAO,** [a,b] **T. R. YU,** [a,b] **B. JELFS,** [b,c] **J. YAN,** [b†] **R. H. M. CHAN** [b,c] **AND Y. LI** [a,b*]

[a] *Department of Biomedical Sciences, City University of Hong Kong, Hong Kong, China*

[b] *Centre for Biosystems, Neuroscience and Nanotechnology, City University of Hong Kong, Hong Kong, China*

[c] *Department of Electronic Engineering, City University of Hong Kong, Hong Kong, China*

Abstract—The rodent anterior cingulate cortex (ACC) is critical for visceral pain and pain-related aversive response in chronic visceral hypersensitive (VH) state. Long-term potentiation (LTP), induced by theta burst stimulation (TBS) in the medial thalamus (MT)-ACC pathway, is blocked in VH rats. However, the neuronal intrinsic firing characteristics and the MT-ACC connectivity have not been investigated in visceral pain. Using repetitive distension of the colon and rectum (rCRD) as a sensitization paradigm, we have identified that the spontaneous firing rates of ACC neurons and the CRD-stimulated neuronal firings were increased after repetitive visceral noxious stimulation. This correlates with increases in visceral pain responses (visceromotor responses, VMRs). Two multichannel arrays of electrodes were implanted in the MT and ACC. Recordings were performed in free-moving rats before and after repeated CRD treatment. Power spectral density analysis showed that the local field potential (LFP) recorded in the ACC displayed increases in theta band power (4–10 Hz) that were modulated by rCRD. Neural spike activity in the ACC becomes synchronized with ongoing theta oscillations of LFP. Furthermore, cross correlation analysis showed augmented synchronization of thalamo-ACC theta band LFPs, which was consistent with an increase of neuronal communication between the two regions. In conclusion, these results reveal theta oscillations and theta-frequency phase-locking as prominent features of neural activity in the ACC and a candidate neural mechanism underlying acute visceral pain.

Key words: anterior cingulate cortex, phase-locking, thalamocortical synchronization, theta oscillation, visceral pain.

INTRODUCTION

Human brain imaging studies (Mayer et al., 2006) and growing experimental evidence have revealed new roles of cortical neuronal networks in chronic visceral pain (Zhuo, 2008; Wang et al., 2013). Hypersensitivity to visceral distention has been reported in patients with irritable bowel syndrome (IBS). Previous studies using functional magnetic resonance imaging showed increases in neuronal activation in the dorsal anterior cingulate cortex (ACC) of patients with IBS. A decrease of this pattern is accompanied by reduction of symptoms of IBS (Mertz et al., 2000). Previously, our electrophysiological studies have shown an increase in *N*-methyl-D-aspartate (NMDA)-receptor activation of ACC neurons (Cao et al., 2008; Wu et al., 2008). Visceral pain behavioral studies have also shown that NMDA-receptor activation plays a causative role on long-lasting visceral pain responses, which are independent of inflammation in the colon in the VH rats (Gao et al., 2006; Fan et al., 2009). Behavioral studies have further demonstrated that ACC activation is critical for the memory processing involved in long-term negative affective states (Yan et al., 2012). Recently, we have characterized the facilitation of synaptic transmission in the MT-ACC pathway, but suppressed long-term potentiation (LTP) induced by electrical stimulation (theta burst stimulation, TBS) in viscerally hypersensitive (VH) rats (Wang et al., 2013). Taken together, these observations suggest that the ACC is a component of a functional circuit that mediates pain perception and processing. However, the underlying neural firing characteristics and synchronized activity are not completely understood in visceral pain.

The theta band (defined between 4 and 10 Hz) has been acknowledged for a wide span of cognitive

*Correspondence to: Y. Li, Department of Biomedical Sciences, Centre for Biosystems, Neuroscience and Nanotechnology, City University of Hong Kong, Tat Chee Avenue, Kowloon, Hong Kong, China. Tel: +852-3442-2669; fax: +852-3442-0522.

E-mail address: yingli@cityu.edu.hk (Y. Li).

† Current address: Faculty of Mental Health, Second Military Medical University, Shanghai, China.

Abbreviations: ACC, anterior cingulate cortex; ANOVA, analysis of variance; AUC, area under the curve; CRD, colorectal distension; IBS, irritable bowel syndrome; LFP, local field potential; LTP, long-term potentiation; MT, medial thalamus; NMDA, *N*-methyl-D-aspartate; rCRD, repetitive colorectal distension; SFC, spike-field coherence; STA, Spike-triggered average; TBS, theta burst stimulation; VH, viscerally hypersensitive; VMR, visceromotor response.

http://dx.doi.org/10.1016/j.neuroscience.2015.04.024

functions, such as: focused attention (Ishii et al., 1999), encoding new information (Klimesch, 1999) and increased memory-load (Jensen, 2005) as well as pain perception (Tai et al., 2006). In humans, theta band activity is mostly generated by structures of the limbic system such as the hippocampus and the cingulate cortex, as well as the prefrontal cortex (Raghavachari et al., 2006). The theta band has also been acknowledged for pain perception. Animal studies using depth electrodes on the cingulate cortex detected theta rhythms in rats (Nishida et al., 2004) and in cats (Calvo and Fernandez-Guardiola, 1984). Furthermore, human studies have shown that both experimentally induced acute and chronic pain perceptions can be influenced by transcranial magnetic TBS. In healthy individuals, painful stimulation in the hand resulted in subjective reports of pain, continuous inhibitory TBS paradigm applied over the contralateral insular and ACC reduced pain perception, and further altered the local field potentials (LFPs) during pain processing (Csifcsak et al., 2009; Antal and Paulus, 2010).

It has been speculated that low-frequency cortical oscillations in the thalamocortical connection play a role in pain perception (Walton et al., 2010; Schulman et al., 2011). Painful sensory experiences modulate thalamocortical oscillations. However, evidence in the literature is controversial. Electrophysiological recordings in patients with neurogenic pain revealed increased synchrony in thalamocortical oscillations (Sarnthein and Jeanmonod, 2008), whereas a functional magnetic resonance imaging study showed that thalamocortical oscillations are desynchronized in a rat model of central pain (Seminowicz et al., 2012). However, the neuronal intrinsic firing characterizes, and the MT–ACC connectivity has not been investigated in visceral pain.

Conditioning jejunal distension increases the perception of discomfort in healthy human volunteers (Serra et al., 1995). In patients with IBS, repetitive colorectal distention (rCRD) has been reported to induce visceral hypersensitivity (Munakata et al., 1997; Saito-Nakaya et al., 2008). In this study we use an animal model of rCRD to facilitate short-term visceral pain response. We hypothesize that repeated visceral noxious stimuli sensitize ACC neurons, augment phase-locking of spikes and ongoing field potential theta oscillations, and further facilitate the synchrony between the MT and ACC.

Multiple-electrode array recording of LFP was performed. Power spectral density analysis showed increases in accumulative power of the theta band in the ACC in rCRD rats. To measure the phase synchronization between spikes and field potential oscillations, we quantified the spike-field coherence (SFC). To clarify the significance of phase-locking of spikes with the theta oscillation, the phase distribution and Rayleigh test were performed. Finally, cross correlation analysis showed augmented synchronization of thalamocortical theta band LFPs is consistent with increases of neuronal communication between the two regions. These results reveal theta oscillations and theta-frequency phase-locking in the ACC are a candidate neural mechanism underlying acute visceral pain. Synaptic transmission at the MT-ACC synapse was better synchronized in visceral pain.

EXPERIMENTAL PROCEDURES

Animals

Unless otherwise stated, all chemicals were purchased from Sigma–Aldrich (Tin Hang Ltd, HK). Experiments were performed on adult male Sprague–Dawley rats (250–350 g). The animals were kept in their home cages and maintained on a 12:12-h light:dark cycle and provided with food and water *ad libitum* for at least five days before use. All surgical and experimental procedures were approved by the Committee on Use and Care of Animals at the City University of Hong Kong and the licensing authority of the Department of Health of Hong Kong to conduct experiments (No. 14-44 in DH/HA&P/8/2/5).

Viscerally hypersensitive rat model: rCRD

The detailed procedures of the CRD were described in our previous publications (Cao et al., 2008; Wang et al., 2013). In brief, polyethylene tubing was attached to a 4.0-cm long balloon. The inflating device was inserted through the anal canal 10 cm down the rectum, and the tube was secured to the base of the tail. CRD pressures were produced by rapidly injecting saline into the balloon over 1 s. A sensitized paradigm consisting of repetitive phases of CRD (80 mmHg maintained for 30 s, repeated eight times with a 1-min interval) was delivered to the rats. The control group received the same treatment but with non-nociceptive colorectal stimulation (20 mmHg). All procedures were performed under conscious condition.

Visceromotor response (VMR) to CRD

Details of the procedures were described previously (Fan et al., 2009; Wang et al., 2013). Briefly, Teflon-coated 32-gauge stainless steel wires were implanted into the external oblique pelvic muscles to monitor the number of abdominal muscle contractions. Graded-pressure CRDs (20, 40, 60 and 80 mmHg) were applied to establish stimulus–response curves. Each CRD pressure was tested three times with 4-min intervals to get a stable response. The results of electromyography were quantified by calculating the area under the curve (AUC).

Multiple-channel recording in free-behaving rats

Rats were anesthetized with pentobarbital (i.p. 50 mg/kg) and placed in a stereotaxic frame. A midline scalp incision was made to expose the skull then two small holes (1–2 mm wide) were drilled above the selected implantation sites of recording electrodes, and then the bone and dura were removed. The animals were inserted with two 16-channel microwire electrode arrays (Plexon, Dallas, TX, USA) in the cingulate cortex area 1 and 2 of the ACC (AP 2.5–3.0, ML 0.6–1.0 mm, depth 1.5–3.5 mm) and the ipsilateral central lateral and mediodorsal lat of the medial thalamus (MT, AP −3.5 to −4.0, ML 1.0–1.5, depth 5.0–7.0 mm). The silver

grounding wires from the recording electrodes were wrapped around the mounting screws. The recording electrodes were advanced slowly into the brain using a micropositioner until the clear neuronal firings in most recording channels were observed on-line (OmniPlex® D system, Plexon, Dallas, TX). A mixture of mineral oil and bone wax was packed around the electrode penetration zone. Electrodes were secured to the rat's skull using dental cement. After the surgery, rats were injected with buprenorphine (0.1 mg/kg) as an analgesic, and 1.0 ml sterile saline for hydration (Steenland et al., 2012), then placed on a warm heating pad for recovery. After a 6–8 day recovery, rats were allowed to adapt to the recording environments and were handled for 3–5 min daily for 2–3 days. The LFPs and spike firings were recorded simultaneously using 64-channel OmniPlex® D Neural Data Acquisition System (Plexon Inc., Dallas, TX). LFPs were amplified (×20,000), band-pass filtered (0.05–200 Hz, 4-pole Bessel) and sampled at 1 kHz. Spikes were filtered (0.3–5 kHz, 4-pole Bessel) and sampled at 40 kHz. All procedures were performed during the light phase. Neural recordings were obtained in their home cages during quiet states. Data were recorded before rCRD treatment, 15 min, 2 h, 4 h and 6 h after rCRD cessation.

Histological identification of stimulated and recorded sites

After completion of the electrophysiological recordings, a DC current (100–500 μA) for 5–10 s was passed sequentially between the recording electrodes and ground to lesion the brain and then rats were anesthetized with isoflurane. Rats were perfused with saline followed by 4% paraformaldehyde. Brain were sliced at 50 μm using a freezing microtome and stained with Cresyl violet. Drawings were made of sections showing electrode tracks related to the structure of the ACC and MT. A standard rat atlas (Paxinos and Watson, 2014) was used as reference for reconstruction of the stimulating and recording sites (Gao et al., 2006).

Statistical analysis

Results of the VMR studies at different time points of rCRD or control treatment were compared by a two-way ANOVA, followed by multiple comparisons adjusted by the Bonferroni's test. The multi-channel neural data were processed off-line using NeuroExplorer 5 (Plexon, Dallas, TX) and exported to custom-written MATLAB (MathWorks, Natick, MA, USA) programs for additional analysis. The data sets were compared by a two-way repeated-measures ANOVA, followed by Bonferroni's test. Results were expressed as mean ± SEM. $p < 0.05$ was considered statistically significant.

Multiple-channel neural data analyses

Spike sorting. The single-unit spike sorting was conducted by Off-Line Spike Sorter V3 software (OFSS, Plexon Inc., Dallas, TX) using combined automatic and manual sorting methods. All waveforms recorded from each channel were isolated as distinct clusters in 3D space based on the characteristics of spike waveforms using principal component analysis (PCA). Automatic techniques were used to generate separation of waveforms into individual clusters. Manual checking was performed to ensure that the spike waveforms were consistent and cluster boundaries were clearly separated. Spikes were identified when a minimum waveform amplitude threshold of 3SDs higher than the noise amplitude was detected. All isolated single-units exhibited recognizable refractory periods ($\geqslant$1 ms) in the inter-spike interval (ISI) histograms (Steenland et al., 2012). After sorting, a single unit was deemed responsive to colorectal distension (CRD) if its spike firing rate increased at least 10% from its pre-distension baseline.

Spectral analysis. Brain oscillations in the theta (4–10 Hz) range are believed to temporally link single neurons into assemblies cooperatively facilitating synaptic plasticity (Buzsaki and Draguhn, 2004). To identify alterations in the theta power spectra following the rCRD paradigm, we characterized the ACC theta power as well as theta ratio (theta/(theta + delta). In order to achieve this, the raw ACC LFPs were filtered between 1 and 100 Hz using non-causal zero-phase-shift filter (fourth-order Butterworth). Then the power spectral densities (PSD) were calculated by multi-taper estimates with seven tapers, 2^{13} frequency bins in the range [0, 500 Hz] (NeuroExplorer 5, Plexon, Dallas, TX) and 50% overlapping windows (window durations were 2^{14} data points). The PSD curve was smoothed with a Gaussian filter (15 bins running average). The band power was defined as the area under the curve of the corresponding frequency domain. 30-s segments of LFP data during spontaneous activity and visceral stimulating condition from each animal were used to calculate the PSD, and the PSD values from each animal were averaged over the 16 channels in the ACC. To compute the theta/delta ratio, the AUC of the theta band power to the theta plus delta band (1–10 Hz) was calculated. To investigate the time–frequency relationships of the theta oscillations in both MT and ACC, the time-varying power spectra were calculated by FFT with a Hann window function using NeuroExplorer 5. The spectrum units were normalized by raw PSD, so that the sum of all the spectrum values equals to the mean squared value of the signal.

Computing the coherence between spikes and LFP. A growing body of research suggests that neuronal signal processes not only in terms of the firing rates of neurons but also by varying the timing of spikes relative to large-scale neuronal oscillations. The temporal coding is critical in memory and perception. To measure the phase synchronization between spike and field potential oscillations, we quantified the SFC (Rutishauser et al., 2010). First, for every spike, a segment of the LFP data centered on the spike ±480 ms long was extracted. The spike-triggered average (STA) was calculated as the mean of all these sections. Then the frequency spectrum of the STA (*f*STA) was calculated using multitaper analysis which uses a series of discrete prolate spheroidal

sequences (seven tapers) to give estimates of the PSD. The same method was then used to calculate the frequency spectra of each of the traces individually. The average of these individual frequency spectra results in the spike triggered power as a function of frequency STP(f). Finally, the SFC was calculated as the *f*STA over the STP(f) as a percentage. SFC(f) = [*f*STA(f)/STP(f)] * 100%. As the SFC is influenced by the number of spikes in the calculation, we equalized the number of spikes in compared groups by randomly selecting a subsample of spikes from the larger group.

The phase-locking of single neurons to the theta oscillation. To explore the angular distributions of spikes in relation to their ongoing theta oscillation, and clarify the significance of the phase-locking, we plotted the phase distribution and performed the Rayleigh test using custom-made MATLAB scripts modified on a elegant study (Rutishauser et al., 2010). To ensure the validity of the statistical results, only neurons which had at least 50 spikes were used for phase-locking estimation. Before performing the computation, 22 frequencies ranging from 1.6 to 64 Hz were selected, such that, $f = 2^x$ with $x = \{6/8, 8/8, 10/8, 12/8, \ldots, 48/8\}$. The LFP was then convolved with a series of Morlet wavelets centered at each of the selected frequencies and with a length of four cycles. The result of these wavelet transforms, is a matrix of vectors whose absolute values (or length) and arguments (or angles) represent the amplitude and phase, respectively, of the LFP at frequency *f* and time *t*. The circular mean of the spike phases was calculated by taking the weighted sum of the cosine and sine of the angles. The mean angle was then the angle of the results and the mean vector length (*R*) the absolute value over the number of spikes. To check for phase-locking, the Rayleigh test was used to compare against uniformity by calculating the test statistic and a *p* value. A neuron was considered phase locked if the *p* value was below the threshold of 0.0023 which is 0.05 Bonferroni corrected for multiple comparisons (0.05/22, twenty-two frequencies were tested) (Rutishauser et al., 2010).

Synchronized theta oscillations between MT and ACC. Synchronized theta activities between the MT LFP_θ and ACC LFP_θ were evaluated by cross-correlograms using NeuroExplorer 5 software. We aligned the 2 LFP_θs and chose the MT LFP_θ as reference. Pearson correlation values were calculated with a lag time ranging from −0.5 to 0.5 s with small bins (2 ms). The cross-correlation curves were smoothed with a Gaussian filter (5 bins running average). We averaged the cross-correlograms from valid electrode channels in the MT and ACC and took the second positive peak as a quantitative measure because it locates at about a 0.2-s lag time which represents theta activity at about 5 Hz (Jeon et al., 2010).

RESULTS

Increased VMRs to CRD following rCRD treatment

A total of eight rCRD and five control rats were tested. The VMR to graded CRDs were measured in rats in the pre-repeated CRD treatment and 15 min, 2 h, 4 h and 6 h after rCRD. Both control and rCRD rats showed pressure-dependent increases in the VMR to CRD. Original recordings of electromyography (EMG) are shown in Fig. 1A. A significant VMR to the lowest distention pressure tested (20, 40 mmHg) in the rats after rCRD, and an absence of response to the lowest distention pressure in the baseline suggest a reduction of pressure threshold (i.e., allodynia) in the following rCRD. Graded CRD pressures of 40, 60, and 80 mmHg caused marked increases in the EMG mean amplitude (AUC) volumes after rCRD treatments compared with the pre-rCRD volumes ($F_{(4,35)} = 13.84$, $p < 0.001$; Fig. 1B) suggesting that repeated noxious CRD stimuli lead to visceral hypersensitivity in rats. *Post hoc* analysis revealed that VMR increased at 15 min, 2 h and 4 h but recovered at 6 h after rCRD compared to pre-rCRD (Fig. 1B). In contrast, in control rats, various CRD pressures induced no significant VMR responses at different time points compared with pre-control treatment ($F_{(4,25)} = 1.28$, $p > 0.05$; Fig. 1C).

Enhanced ACC neuronal activities in free-moving rats

In control rats ($n = 7$), a total of 211 neurons were isolated with 51 neurons (24.2%) showed excited response to 60 mmHg CRD. In rCRD treatment rats ($n = 9$), 63 of 245 neurons (25.7%) were deemed as CRD-excited neurons. An example of a spike-firing rate histogram of a CRD-excited neuron is shown in Fig. 2A. A two-way ANOVA revealed a main effect of time points following rCRD ($F_{(4,310)} = 9.62$, $p < 0.001$; Fig. 2B). The average spontaneous firing rate recorded in the CRD-excitatory neurons were significantly increased at 15 min and 2 h after rCRD (3.71 ± 0.76 and 3.49 ± 0.31 spikes/s at 15 min and 2 h respectively; versus 2.10 ± 0.24 spikes/s pre-rCRD; $t = 2.62$ and 2.3 respectively, $p < 0.05$). ACC neuronal responses to 60 mmHg CRD increased from pre-rCRD (3.27 ± 0.29 spikes/s) to 6.03 ± 0.49, 5.58 ± 0.59 at 15 min and 2 h ($t = 4.52$ and 3.85 respectively, $p < 0.001$, respectively). In the control group the ACC neural responses to both spontaneous and CRD conditions remain unchanging at different time points ($F_{(4,250)} = 0.94$, $p > 0.05$; Fig. 2C). These observations demonstrate that rCRD rats have a reduction of CRD pressure threshold and an increased ACC neuronal excitability.

Augmented ACC theta activity after rCRD paradigm

Power spectral analysis was performed to compare the ACC theta oscillation power of LFPs before rCRD, 15 min, 2 h, 4 h and 6 h after rCRD cessation. Averages of the Fourier transform for spontaneous field potentials at different time points are depicted in Fig. 3A. The AUC of theta band power in both spontaneous and CRD conditions in rCRD rats is shown in Fig. 3B ($n = 9$). A significant alteration was detected ($F_{(4,40)} = 6.31$; $p < 0.001$; two-way ANOVA). *Post hoc* analysis revealed that spontaneous theta band power increased from 0.0018 ± 0.00012 at pre-rCRD to 0.0022 ± 0.00005 and

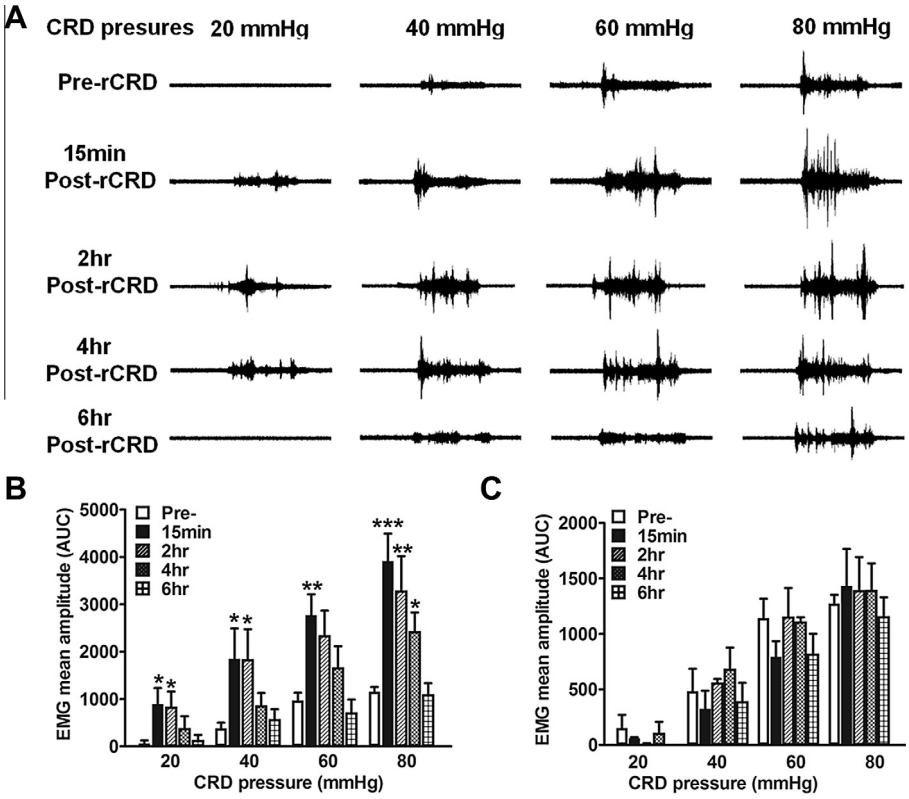

Fig. 1. The visceromotor response (VMR) to colorectal distension (CRD) was facilitated following repetitive CRD (rCRD) treatment. (A) Representative EMG recordings to graded CRD pressures (20, 40, 60 and 80 mmHg) in normal rats at pre-, 15 min, 2 h, 4 h and 6 h post-rCRD. (B) EMG mean amplitudes (AUC) in response to graded CRDs were significantly increased after rCRD treatment; this enhancement of visceral pain response was recovered at 6 h post-rCRD. (C) Same as (B) but for control rats. Results are presented as mean ± SEM. Statistical significance was determined by a two-way ANOVA, followed by the Bonferroni's test, $^{*}p < 0.05$, $^{**}p < 0.01$ and $^{***}p < 0.001$.

$0.0021 \pm 0.00003\ mV^2$ at 15 min and 2 h ($t = 2.70$ and 2.65 respectively; $p < 0.05$), but was not significantly changed at 4 h and 6 h after rCRD ($t = 0.23$ and 0.26 respectively; $p > 0.05$) compared with pre-rCRD. Theta ratios were also evaluated in the current study (Fig. 3C). *Post hoc* analysis revealed that in spontaneous condition ACC theta ratio was enhanced from 46.29 ± 2.08 to 56.84 ± 1.18 and 56.62 ± 1.13% at 15 min and 2 h ($t = 2.75$ and 2.69 respectively; $p < 0.05$). During CRD the theta ratio was also increased from 54.43 ± 2.50 in pre-rCRD treatment to 64.94 ± 1.83% at 2 h after rCRD ($t = 2.62$; $p < 0.05$). No significant changes of theta band power were observed in the control group ($F_{(4,30)} = 1.25$, $p > 0.05$; Fig. 3D). These data suggest that rCRD modulates spontaneous, and the visceral noxious stimulation-induced ACC theta activities.

Facilitated spike field coherence in the ACC after rCRD treatment

The SFC was used to quantify the spike timing–LFP relationship alteration in rCRD-treated rats. The SFC value is expressed in percentage and varies as a function of frequency. The SFC value varies among 0% to 100%, 100% indicates all spikes following a particular phase of oscillation in this frequency while 0 reflects spikes firing completely at random In the present study we computed SFC values of all CRD-excited neurons at both resting and CRD stimulations, the SFC distributions during the spontaneous condition at various time points following rCRD are presented in Fig. 4A. We found a significant difference of the average SFC in 4–10 Hz range among 5 time points in rCRD rats ($F_{(4,310)} = 5.01$, $p < 0.001$; Fig. 4B). *Post hoc* analysis revealed that SFC values of both spontaneous and CRD conditions were increased at 15 min, 2 h and 4 h but not at 6 h after rCRD compared to pre-rCRD condition. In the control group, there was no significant change among various time points ($F_{(4,250)} = 0.12$, $p > 0.05$; Fig. 4C). These results suggest that the increased SFC of CRD-excited neurons in the ACC corresponded to the rCRD treatment.

Increased proportions of phase-locked neurons in the ACC following rCRD

Oscillatory firing of neurons does not necessarily lead to oscillatory LFPs, and oscillatory neuronal firing is not necessarily synchronous with the LFP. To further investigate the strength of coupling between spike timing and LFP at any given frequency, we next asked whether spike phase distributions in the local theta oscillation of LFPs were changed in rats after rCRD treatment. As expected, we found that at pre-rCRD 11.84% of neurons (29 of 245 neurons) fired spikes that were phase-locked to the LFP oscillations in the theta

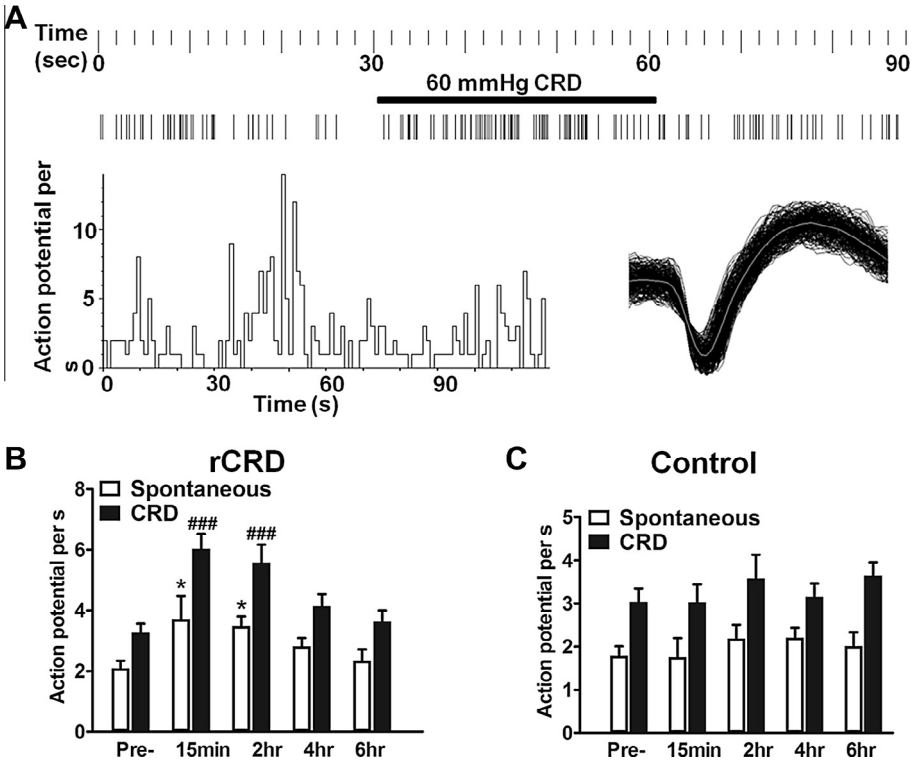

Fig. 2. The neuronal firing rates of CRD excited ACC-neurons were increased in rCRD rats. (A) An example of CRD- excited neuron. Upper: Spike time stamps of CRD-excited ACC neuron from a normal rat before rCRD training, 60 mmHg CRD was administrated during 30–60 s. Lower: Spike firing rate histogram, left; and the corresponding spike waveforms are shown in the right. (B) Averaged spike firing rates of all CRD-excited ACC neurons show the firing rates in both spontaneous and during 60 mmHg CRD stimulation were increased at 15 min and 2 h after rCRD treatment. (C) Same as (B) but for control rats. Statistical significance was determined by a two-way ANOVA, followed by the Bonferroni's test, *represents significant changes in the spontaneous condition compared with pre-rCRD, $p < 0.05$; ###for the CRD condition, $p < 0.001$.

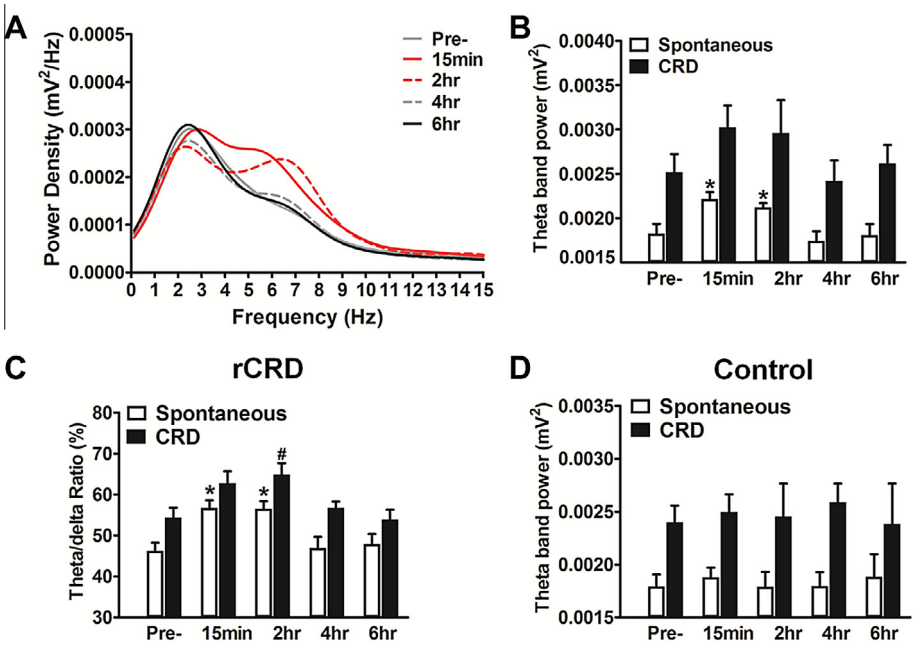

Fig. 3. The theta band oscillation (4–10 Hz) power in the ACC was enhanced following rCRD stimulation. (A) The mean power spectral density (PSD) plots in spontaneous condition at pre-, 15 min, 2 h, 4 h and 6 h post-rCRD, showing the enhancement of the PSD at 15 min and 2 h post-rCRD treatment. (B) The histogram shows the theta-band power (AUC) was enhanced in the spontaneous LFP at 15 min and 2 h post-rCRD compared with pre-rCRD treatment. (C) The histogram shows the theta ratio (theta/(theta + delta)) was enhanced during both spontaneous and 60 mmHg CRD at 15 min and 2 h after rCRD treatment. (D) Same as (B) but for control rats. Results are presented as mean ± SEM. Statistical significance was determined by a two-way ANOVA, followed by the Bonferroni's test, *represents significant changes in the spontaneous condition compared with pre-rCRD, $p < 0.05$; #for the CRD condition, $p < 0.05$.

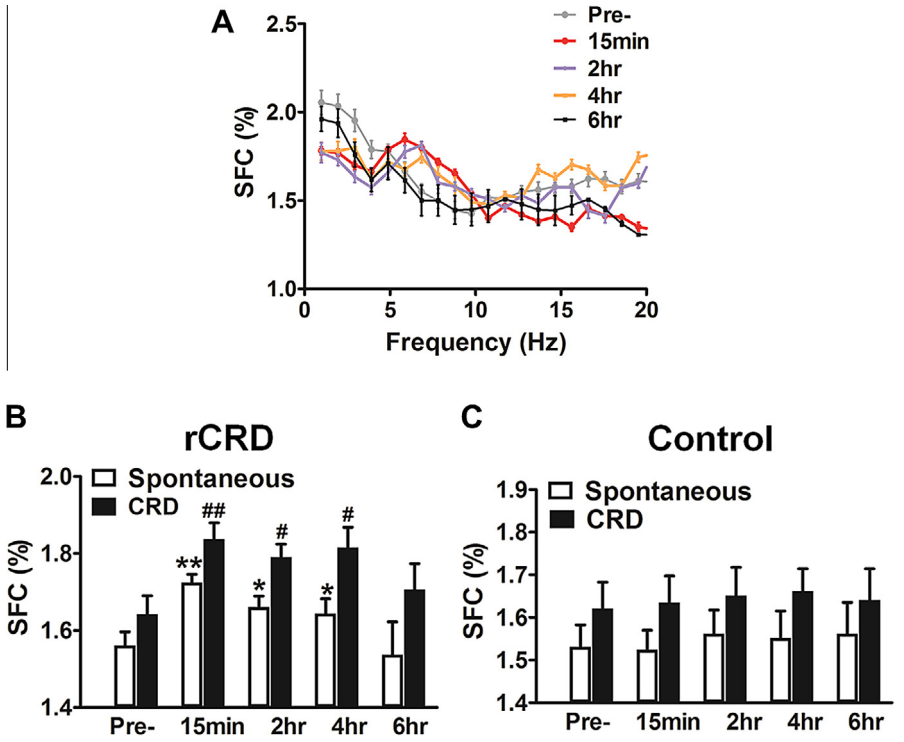

Fig. 4. The coherence between spikes and the theta oscillations was increased after the rCRD paradigm. (A) Distribution of the spike field coherence (SFC) spectrum in spontaneous conditions at pre-, 15 min, 2 h, 4 h and 6 h post-rCRD treatment. (B) The mean SFC values in the theta band were increased indicating that the spike-field relationship in both spontaneous and CRD conditions were strengthened at 15 min, 2 h and 4 h post-rCRD. (C) Same as (B) but for control rats. Data are expressed as mean ± SEM. * and **represent significant changes in the spontaneous condition compared with pre-rCRD, $p < 0.05$ and $p < 0.01$ respectively; # and ##for the CRD condition, $p < 0.05$ and $p < 0.01$ respectively.

range (Fig. 5A, $p < 0.0023$, 0.05/22, Rayleigh's test). In contrast, at 15 min, 2 h, 4 h and 6 h after rCRD, 18.4% (45 of 245 neurons), 20.0% (49 of 245 neurons), 19.2% (47 of 245 neurons) and 10.6% (26 of 245 neurons) respectively showed phase-locking at the theta range. Examples of phase distributions of a phase-locked neuron and a un-phase-locked neuron are presented as polar-histograms (Fig. 5B, C). The phase-locked neuron in Fig. 5B showed most spikes firing at between 270° and 360° of the theta cycle with a mean-phase of 290°. However, the un-phase-locked neuron displayed random firing. The preferred theta phase distributions of phase-locked neurons at various time points are shown in Fig. 5D. Together, the results indicate the enhanced strength of spike phase-locking of single neuron spikes in relation to ongoing LFP in rCRD rats. These observations also indicate that the LFPs are not 'contaminated' by the unit activity and further suggest that the LFPs recorded from the microelectrodes are much more likely to reflect synchronized inputs to the neurons (e.g., dendritic membrane oscillations) rather than axonal spiking activity.

Synchronized theta activity in ACC and MT after rCRD treatment

The cortex is driven by weak but synchronously active thalamocortical synapses (Bruno and Sakmann, 2006). To identify the functional connectivity between MT and ACC, we simultaneously recorded LFPs in MT and ACC in conscious rats, we compared the LFPs during a 30-s spontaneous and 30-s CRD stimulation before rCRD treatment, and 15 min, 2 h, 4 h and 6 h after rCRD treatment. Time-varying power spectral analysis of 120-s recordings revealed that the moderate and dispersed brain oscillations in the MT and ACC in pre-rCRD became intensive and concentrated activities at theta frequency at 15 min after rCRD (Fig. 6B). Cross-correlation analysis (Seidenbecher et al., 2003; Jeon et al., 2010) during spontaneous activities at varied time points of rCRD are shown in Fig. 6C. By averaging the cross-correlograms and taking the second positive peak as a quantitative measure, a significant synchronized theta rhythm between the MT and ACC in rCRD rats was detected ($F_{(4,40)} = 38.05$; $p < 0.001$, two-way ANOVA; Fig. 6D). *Post hoc* analysis revealed that the second peaks of correlation value in both spontaneous and 60 mmHg CRD conditions were increased at 15 min, 2 h and 4 h but recovered at 6 h after rCRD treatment (Fig. 6D). In contrast in the control group there is no difference among different time points of treatment ($F_{(4,30)} = 2.37$; $p > 0.05$, two-way ANOVA; Fig. 6E). The synchronized theta activities between ACC and MT after rCRD treatment suggests an increased dynamic information transfer between them.

DISCUSSION

In this study we report how induction of acute visceral pain affects the patterns of MT-ACC activity by

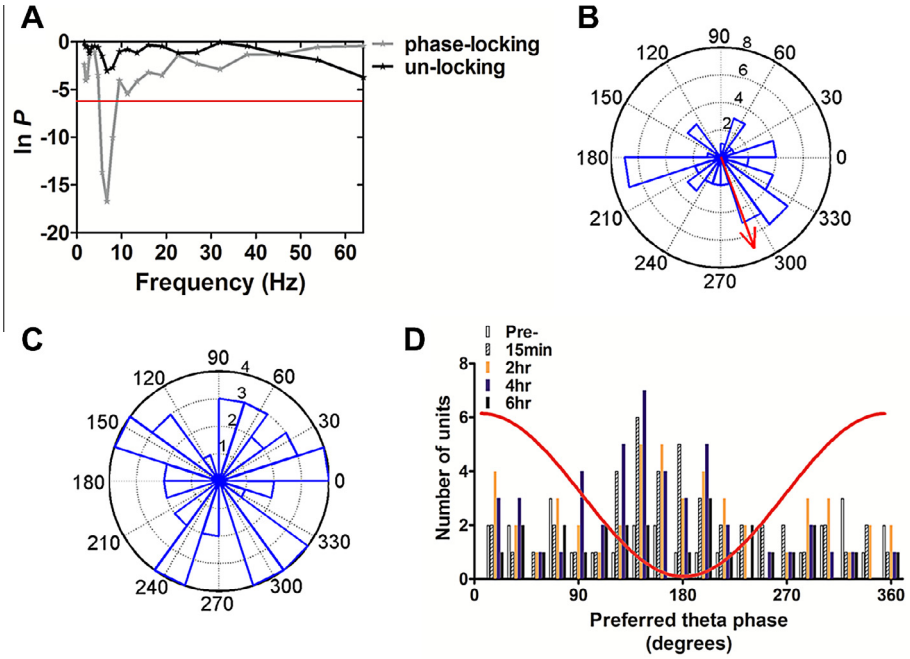

Fig. 5. The spike phase-locking to the theta oscillation in the ACC. (A) Test of significance of phase-locking as a function of frequency (1–64 Hz). The threshold (red line) for significant phase-locking was set to $p = 0.0023$ (0.05/22, Bonferroni corrected). The shown phase-locked neuron (gray line) exhibited maximal phase-locking at 6.7 Hz while the un-phase-locked neuron (black line) showed no significant phase-locking in the theta range. (B) The polar-histogram of the spike-field phase distribution of the phase-locked neuron shown in (A). The figure shows the majority of spikes of this neuron fired close to 300°. The mean phase shown by the red arrows indicates this neuron preferred firing at 290° of the theta oscillation. The vector length $R = 0.34$. (C) Polar-histogram of the spike-field phase distribution of the un-locked neuron shown in (A). The figure shows this neurons action potential firing at random angles of the theta cycle oscillations. The vector length $R = 0.03$. (D) Histogram of the preferred phase of all phase-locked neurons distribution in the rCRD rats at pre-, 15 min, 2 h, 4 h and 6 h post-rCRD. The figure shows most phase-locked neurons preferred to fire during the descending phase or at the trough of the oscillation. The red line is a schematic of the theta cycle.

examining LFP activity in rats following repeated visceral noxious stimulation. The behavioral task used in the present study is a well-established visceromotor reflex to assess visceral pain. Multiple-channel recordings of LFP in ACC and MT were conducted in conscious rats. Power spectral density analysis displayed increases in accumulative power of the theta band (4–10 Hz) in the ACC, which were modulated by rCRD. Neural spike firings in the ACC become synchronized with ongoing theta oscillations of LFP. Furthermore, cross correlation analysis showed augmented synchronization of the thalamo-ACC theta band LFP is consistent with increases of neuronal communication between the two regions.

It has been reported that repetitive noxious CRD increases Fos immunoreactivity in the spinal cord via N-methyl-D-aspartate receptors (Zhai and Traub, 1999). However, the brain targets for the repetitive noxious stimulations induced visceral hypersensitivity have not been characterized. ACC neurons responded to visceral stimulation. We have reported, previously, that only 24% of ACC neurons showed a mild increase in firing rates in response to 60 mmHg CRD (Gao et al., 2006). These data suggested that ACC visceral nociceptive neurons are not easily excitable under normal conditions. In this study, however, the rats followed repeated CRD treatment at the spontaneous firing rate, and the CRD-evoked ACC neural firings were higher compared with pre-rCRD condition suggesting sensitization of the ACC. Measuring behavioral visceral pain we showed that the rCRD condition enhanced visceral pain responses, which lasted for 240 min.

In the past few years it has become increasingly acknowledged that large-scale oscillatory activity plays an important role in basic brain function. Electrophysiological studies from animals have revealed that ACC neurons are likely to fire spikes at about 4–10 Hz (theta) during different behavioral tests (Nishida et al., 2004). Proportionately, more brain neuronal theta activity predicts faster and better learning. The learning process induces enhancement of theta activity during training in animals (Hoffmann and Berry, 2009). Compared with gamma oscillation, theta oscillation was much less investigated in neural disorders. Recently, we have shown significant increases in LFP in the sensitized rat, suggesting enhancement of synaptic transmission in the thalamo-ACC synapses; this is mediated by both NMDA and AMPA receptors (Wang et al., 2013). Further, TBS in the MT reliably induced LTP in the MT-ACC pathway in normal rats. However, induction of visceral hypersensitivity effectively blocks the expression of LTP at thalamo-ACC synapses *in vivo* supporting the notion that visceral hypersensitivity and electrically induced LTP share common mechanisms. To further characterize whether LTP-like synaptic plasticity in the MT-ACC synapses contributes to visceral pain in VH state, we showed that repeated application of theta-patterned tetanization in the MT in the awake normal rats

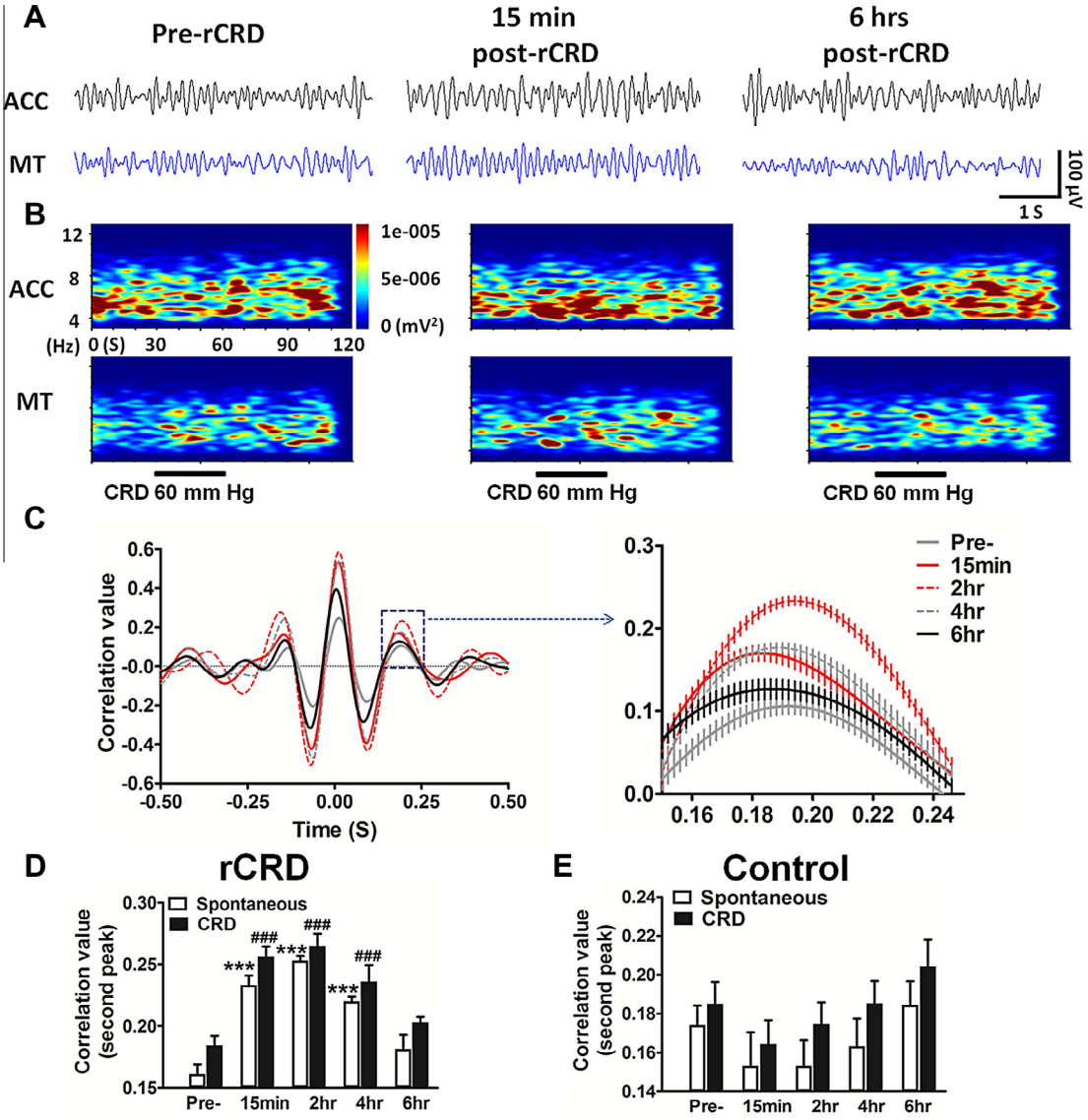

Fig. 6. The theta activities between ~~the~~ ACC and MT were synchronized in response to rCRD treatment. (A) Representative original traces of theta-band LFPs in the ACC (black line) and MT (blue line) during CRD in pre- (left), 15 min (middle) and 6 h post-rCRD treatment (right). (B) Two minutes colored power spectra of LFPs in ACC and MT show synchronized theta oscillations at 15 min after rCRD treatment. (C) The averaged cross-correlograms between ACC and MT theta-band oscillations in spontaneous conditions at different time points of the rCRD paradigm. The second peaks of the cross-correlograms are shown in the right panel. (D) Histograms show the averaged second peaks of cross-correlograms in both spontaneous and 60 mmHg CRD conditions at different time points of rCRD. The enhanced cross-correlation values in both spontaneous and CRD conditions at 15 min, 2 h and 4 h but not 6 h suggesting synchronized theta oscillations between the ACC and MT after rCRD treatment. (E) Same as (D) but for control rats. Results are presented as mean ± SEM. Statistical significance was determined by a two-way ANOVA, followed by Bonferroni's test, ***represents significant changes in the spontaneous condition compared with pre-rCRD, $p < 0.001$; ###for the CRD condition, $p < 0.001$.

resulted in enhancement of CRD-induced ACC responses and facilitation of behavioral visceral pain, which mimicked ACC sensitization and visceral allodynia and hyperalgesia in the VH model as we demonstrated previously (Gao et al., 2006; Cao et al., 2008; Fan et al., 2009). We postulate that visceral hypersensitivity, ACC sensitization, and long-lasting enhanced synaptic transmission in the VH state are expressed by the same core mechanisms as TBS-induced canonical LTP in rats (Wang et al., 2013). In this study, to determine whether repeated noxious visceral stimulation enhances endogenous theta rhythms in area ACC, multiple-electrode array recordings technique was used in freely moving rats. We found that the rats following rCRD treatment exhibited higher spectral power; maximal alterations were observed in the 4–10-Hz theta band in all electrodes. The theta rhythms became substantially stronger in the ACC during visceral noxious stimulation (CRD).

Theta activities induce a fluctuation in the cellular excitability. Enhanced theta oscillations may facilitate the spatially distant and non-interacting neurons fire action potentials simultaneously. Importantly, cross-correlation analysis revealed after repeated CRD training, both resting and CRD-induced LFPs at ACC

and MT became synchronized. Given evidence that theta waves or theta frequency stimulation facilitates synaptic plasticity, the increase in synchronized theta activities in MT-ACC circuits may represent an increase in neuronal communication in these areas (Seidenbecher et al., 2003). The synchronized oscillatory activity facilitates communication and modifies synaptic weights between anatomically distant, but functionally related, structures during learning (Seidenbecher et al., 2003; Buzsaki and Draguhn, 2004). To our knowledge this report is the first demonstration that noxious visceral stimulation induced plastic changes in thalamus-ACC, related to theta rhythms processing. Our data are consistent with the clinical observations that theta-over activation in pain patients was found to be localized in the thalamus, prefrontal medial areas and in the ACC (Stern et al., 2006; Sarnthein and Jeanmonod, 2008). In animal studies, the alteration of theta oscillation has also been reported. The increases in power of theta activity has been clarified in rats with formalin nociception (Tai et al., 2006) and following stressor of restraint or tail shock (Shors et al., 1997).

Visceral pain may cause body movement. It has been demonstrated that the body movement could modulate theta activity in the brain areas including the cingulate cortex (Borst et al., 1987). Notably, the ACC neurons characterized in our current and previous studies were activated by visceral noxious stimulation (Gao et al., 2006; Wu et al., 2008). We have shown that splanchnicectomy combined with pelvic nerve section abolished ACC responses to visceral noxious stimulation in rats. Further, enhanced ACC nociceptive transmission in viscerally hypersensitive rats is restricted to visceral afferent input, but not somatic stimuli (Gao et al., 2006). Therefore, it is conceivable that visceral noxious afferent inputs are major contributors to the altered theta oscillations presented in this study.

Ample evidence suggests that neurons transmit information not only in terms of their firing rates, but also by varying the timing of the spikes corresponding to neuronal oscillations (Varela et al., 2001). The field potential oscillations modulate local spike timing (Jacobs et al., 2007; Frohlich and McCormick, 2010). Further, the induction of synaptic plasticity is favored by coordinated action-potential timing across neuronal networks (Markram et al., 1997), rising oscillations of different frequencies in LFPs. Furthermore, behavioral studies have consistently shown that synchronously discharging cells are more effective at driving neurons at subsequent processing stages than uncoordinatedly responding cells (Hasselmo et al., 2002). A human study has demonstrated that theta-frequency phase-locking of single neurons played an important role in memory strength (Rutishauser et al., 2010). Therefore, we quantified the SFC (Rutishauser et al., 2010) to examine the phase synchronization between spikes and LFP oscillations. The SFC is independent of the LFP power spectrum and the number of spikes, and is therefore immune to changes in these parameters. This allowed us to distinguish between changes in spike-field synchronization and changes in the regularity of oscillatory patterns which are reflected in enhancement of the spectral power of the field potential. Increases in coherence between spikes and theta oscillations in the ACC neurons at rest and during visceral stimulation of rCRD-treated rats were clearly demonstrated in this study. In addition, to advance the understanding of the timing relationship between spikes and ongoing theta oscillation, it is critical to investigate the angular distributions of spikes with the theta oscillation, and clarify the significance of phase-locking of spikes in theta oscillation (Rutishauser et al., 2010). We found that in normal rats before rCRD training, 11.8% of ACC neurons fired spikes that were phase-locked to the LFP oscillations in the theta range. The preferred frequency of phase-locked neurons was 6.7 Hz, with maximal activity during the descending phase and at the trough of the oscillations. In contrast, 20% of ACC neurons showed phase-locking at the theta range at 2 h after the rCRD paradigm. Together, these results suggest that repeated visceral noxious stimulations facilitate phase distribution of ACC neuron spikes in the theta oscillation of LFP.

CONCLUSIONS

We conclude that these findings strengthen the hypothesis that theta oscillations are a prominent feature of neural activity in the thalamo-ACC area in the visceral pain state. The augmented synchronization between thalamus and ACC can be a candidate mechanism underlying visceral pain learning. It will be important for future investigations to electrophysiologically explore the local spike-field interaction, and the synchronized oscillatory activities between MT and ACC to better understand how this system dynamically contributes to a transfer in perceptual learning from acute visceral pain to the chronic visceral pain state.

CONFLICT OF INTEREST

The authors declare that there are no conflicts of interest in the publication of this manuscript.

Acknowledgments—This work was supported by the Research Grants Council of Hong Kong [grant number 11100914 and CityU number 160811, 160812, and 160713 to Y. Li], the Health and Medical Research Fund of Hong Kong [01122006 to Y. Li], the National Science Foundation of China [81170353 to Y. Li], and City University of Hong Kong Neuroscience Research Infrastructure Grant [9610211 to Y. Li]. City University of Hong Kong Centre for Biosystems, Neuroscience, and Nanotechnology Grant (to S. Pang and Y. Li).

We thank Miss Michelle Ye and Professor Georges M. Halpern for editing the manuscript.

REFERENCES

Antal A, Paulus W (2010) Effects of transcranial theta-burst stimulation on acute pain perception. Restor Neurol Neurosci 28:477–484.

Borst JG, Leung LW, MacFabe DF (1987) Electrical activity of the cingulate cortex. II. Cholinergic modulation. Brain Res 407:81–93.

Bruno RM, Sakmann B (2006) Cortex is driven by weak but synchronously active thalamocortical synapses. Science 312:1622–1627.

Buzsaki G, Draguhn A (2004) Neuronal oscillations in cortical networks. Science 304:1926–1929.
Calvo JM, Fernandez-Guardiola A (1984) Phasic activity of the basolateral amygdala, cingulate gyrus, and hippocampus during REM sleep in the cat. Sleep 7:202–210.
Cao Z, Wu X, Chen S, Fan J, Zhang R, Owyang C, Li Y (2008) Anterior cingulate cortex modulates visceral pain as measured by visceromotor responses in viscerally hypersensitive rats. Gastroenterology 134:535–543.
Csifcsak G, Nitsche MA, Baumgartner U, Paulus W, Treede RD, Antal A (2009) Electrophysiological correlates of reduced pain perception after theta-burst stimulation. NeuroReport 20:1051–1055.
Fan J, Wu X, Cao Z, Chen S, Owyang C, Li Y (2009) Up-regulation of anterior cingulate cortex NR2B receptors contributes to visceral pain responses in rats. Gastroenterology 136(1732–1740):e1733.
Frohlich F, McCormick DA (2010) Endogenous electric fields may guide neocortical network activity. Neuron 67:129–143.
Gao J, Wu X, Owyang C, Li Y (2006) Enhanced responses of the anterior cingulate cortex neurons to colonic distension in viscerally hypersensitive rats. J Physiol 570:169–183.
Hasselmo ME, Bodelon C, Wyble BP (2002) A proposed function for hippocampal theta rhythm: separate phases of encoding and retrieval enhance reversal of prior learning. Neural Comput 14:793–817.
Hoffmann LC, Berry SD (2009) Cerebellar theta oscillations are synchronized during hippocampal theta-contingent trace conditioning. Proc Natl Acad Sci USA 106:21371–21376.
Ishii R, Shinosaki K, Ukai S, Inouye T, Ishihara T, Yoshimine T, Hirabuki N, Asada H, Kihara T, Robinson SE, Takeda M (1999) Medial prefrontal cortex generates frontal midline theta rhythm. NeuroReport 10:675–679.
Jacobs J, Kahana MJ, Ekstrom AD, Fried I (2007) Brain oscillations control timing of single-neuron activity in humans. J Neurosci 27:3839–3844.
Jensen O (2005) Reading the hippocampal code by theta phase-locking. Trends Cogn Sci 9:551–553.
Jeon D, Kim S, Chetana M, Jo D, Ruley HE, Lin SY, Rabah D, Kinet JP, Shin HS (2010) Observational fear learning involves affective pain system and Cav1.2 Ca^{2+} channels in ACC. Nat Neurosci 13:482–488.
Klimesch W (1999) EEG alpha and theta oscillations reflect cognitive and memory performance: a review and analysis. Brain Res Brain Res Rev 29:169–195.
Markram H, Lubke J, Frotscher M, Sakmann B (1997) Regulation of synaptic efficacy by coincidence of postsynaptic APs and EPSPs. Science 275:213–215.
Mayer EA, Naliboff BD, Craig AD (2006) Neuroimaging of the brain-gut axis: from basic understanding to treatment of functional GI disorders. Gastroenterology 131:1925–1942.
Mertz H, Morgan V, Tanner G, Pickens D, Price R, Shyr Y, Kessler R (2000) Regional cerebral activation in irritable bowel syndrome and control subjects with painful and nonpainful rectal distention. Gastroenterology 118:842–848.
Munakata J, Naliboff B, Harraf F, Kodner A, Lembo T, Chang L, Silverman DH, Mayer EA (1997) Repetitive sigmoid stimulation induces rectal hyperalgesia in patients with irritable bowel syndrome. Gastroenterology 112:55–63.
Nishida M, Hirai N, Miwakeichi F, Maehara T, Kawai K, Shimizu H, Uchida S (2004) Theta oscillation in the human anterior cingulate cortex during all-night sleep: an electrocorticographic study. Neurosci Res 50:331–341.
Paxinos G, Watson C (2014) The rat brain. 7th ed. San Diego (CA): Academic.
Raghavachari S, Lisman JE, Tully M, Madsen JR, Bromfield EB, Kahana MJ (2006) Theta oscillations in human cortex during a working-memory task: evidence for local generators. J Neurophysiol 95:1630–1638.
Rutishauser U, Ross IB, Mamelak AN, Schuman EM (2010) Human memory strength is predicted by theta-frequency phase-locking of single neurons. Nature 464:903–907.
Saito-Nakaya K, Hasegawa R, Nagura Y, Ito H, Fukudo S (2008) Corticotropin-releasing hormone receptor 1 antagonist blocks colonic hypersensitivity induced by a combination of inflammation and repetitive colorectal distension. Neurogastroenterol Motil 20:1147–1156.
Sarnthein J, Jeanmonod D (2008) High thalamocortical theta coherence in patients with neurogenic pain. NeuroImage 39:1910–1917.
Schulman JJ, Cancro R, Lowe S, Lu F, Walton KD, Llinas RR (2011) Imaging of thalamocortical dysrhythmia in neuropsychiatry. Front Hum Neurosci 5:69.
Seidenbecher T, Laxmi TR, Stork O, Pape HC (2003) Amygdalar and hippocampal theta rhythm synchronization during fear memory retrieval. Science 301:846–850.
Seminowicz DA, Jiang L, Ji Y, Xu S, Gullapalli RP, Masri R (2012) Thalamocortical asynchrony in conditions of spinal cord injury pain in rats. J Neurosci 32:15843–15848.
Serra J, Azpiroz F, Malagelada JR (1995) Perception and reflex responses to intestinal distention in humans are modified by simultaneous or previous stimulation. Gastroenterology 109:1742–1749.
Shors TJ, Gallegos RA, Breindl A (1997) Transient and persistent consequences of acute stress on long-term potentiation (LTP), synaptic efficacy, theta rhythms and bursts in area CA1 of the hippocampus. Synapse 26:209–217.
Steenland HW, Li XY, Zhuo M (2012) Predicting aversive events and terminating fear in the mouse anterior cingulate cortex during trace fear conditioning. J Neurosci 32:1082–1095.
Stern J, Jeanmonod D, Sarnthein J (2006) Persistent EEG overactivation in the cortical pain matrix of neurogenic pain patients. NeuroImage 31:721–731.
Tai SK, Huang FD, Moochhala S, Khanna S (2006) Hippocampal theta state in relation to formalin nociception. Pain 121:29–42.
Varela F, Lachaux JP, Rodriguez E, Martinerie J (2001) The brainweb: phase synchronization and large-scale integration. Nat Rev Neurosci 2:229–239.
Walton KD, Dubois M, Llinas RR (2010) Abnormal thalamocortical activity in patients with Complex Regional Pain Syndrome (CRPS) type I. Pain 150:41–51.
Wang J, Zhang X, Cao B, Liu J, Li Y (2013) Facilitation of synaptic transmission in the anterior cingulate cortex in viscerally hypersensitive rats. Cereb Cortex. http://dx.doi.org/10.1093/cercor/bht273.
Wu X, Gao J, Yan J, Fan J, Owyang C, Li Y (2008) Role for NMDA receptors in visceral nociceptive transmission in the anterior cingulate cortex of viscerally hypersensitive rats. Am J Physiol Gastrointest Liver Physiol 294:G918–G927.
Yan N, Cao B, Xu J, Hao C, Zhang X, Li Y (2012) Glutamatergic activation of anterior cingulate cortex mediates the affective component of visceral pain memory in rats. Neurobiol Learn Mem 97:156–164.
Zhai QZ, Traub RJ (1999) The NMDA receptor antagonist MK-801 attenuates c-Fos expression in the lumbosacral spinal cord following repetitive noxious and non-noxious colorectal distention. Pain 83:321–329.
Zhuo M (2008) Cortical excitation and chronic pain. Trends Neurosci 31:199–207.

(Accepted 11 April 2015)
(Available online 18 April 2015)